Evidence for the Electromagnetic Production of μ Mesons*†

G. E. MASEK AND W. K. H. PANOFSKY
High-Energy Physics Laboratory and Department of Physics, Stanford University, Stanford, California
(Received October 17, 1955)

Direct electromagnetic production of pairs of μ mesons has been investigated. The means of detection chosen consists of searching for the production of single negative μ mesons peaked sharply in the forward direction. The target chosen was aluminum, bombarded by bremsstrahlung from 575-Mev electrons, and the angular range studied was $10°<\theta<30°$. The experimental value of the cross section σ_{exp} was referred to a theoretical value σ_{theor} computed by modifying the conventional formula for the pair production of fermions by photons in a Coulomb field by the introduction of a finite nuclear size. Observations carried out to date give

$$\sigma_{\text{exp}}/\sigma_{\text{theor}}=1.93\pm0.68.$$

The quoted standard error defines the statistical accuracy only and is a measure of the likelihood of existence of the process; in addition, the absolute cross section is uncertain to within a factor of 1.5.

I. INTRODUCTION

THE μ meson is known from its properties to be a particle of rest mass 207 times the electron mass, showing weak interaction with nuclear matter only via the Coulomb field and the Fermi interaction. All known experimental information is compatible with the fact that the spin of the μ meson is half-integral although the proof of this conclusion rests only on the assumed identification of the light neutral particle in $\pi-\mu$ decay, μ^- capture, and $\mu-e$ decay with the neutrino of β decay. In short, the μ meson appears to behave, as far as its scantily known experimental aspects are concerned, exactly analogously to an electron, with the single exception of their different masses. There is some evidence as to anomalous behavior of μ-meson Coulomb scattering[1–8]; also, the question of the detailed identification of the Fermi interaction with the β-decay coupling of nuclei is still uncertain. Clearly, however, there must be some properties that distinguish the interaction of μ mesons from that of electrons. It is, therefore, a matter of considerable importance to attempt to complete a cycle of measurements with the aim of investigating those properties of the μ meson that are inferred by analogy with electrons.

The process of electromagnetic μ-pair production plays a potentially singular role in this connection. Electromagnetic pair production is a second-order electromagnetic process involving (1) interaction of the electromagnetic properties of the muon with the photon field, and (2) scattering, presumed electromagnetic, of the muon in the field of a nucleus. One would expect, in analogy with the electron, the first step to correspond to the coupling of a Dirac current to the incident electromagnetic field, and the second step to Coulomb scattering of muons on a nuclear charge distribution of finite size.

On this basis, a theoretical cross section can be computed which is the Bethe-Heitler formula for electron-positron pair production[9] corrected for finite nuclear size and scaled by the mass differences. Deviations from this "predicted" cross section could result (a) if the coupling of the photon field and the muon electromagnetic properties did not correspond to the muon's being a Dirac particle of normal magnetic moment; (b) if the scattering of the muon in the Coulomb field were anomalous; (c) if there existed alternate means of photoproduction, e.g., predicted by the μ-pair theory of nuclear forces[10]; (d) if more radical assumptions were true, such as the restriction of quantum electrodynamics to coupling the electromagnetic field to electron-positron pairs only, to the exclusion of pairs of other particles.

The experiments on μ-mesic x-rays[11] do not answer all of these questions at this time. Although the experiments have been analyzed with the Dirac equation, the experimental data do not reveal any significant fine structure, and the influence on the bound levels of the negative energy states is not established. Potentially, however, precise measurements on μ-mesic x-rays could serve as evidence for the existence of μ pairs.

Work on the specific problem of the photoproduction of μ-pairs has been carried out previously by Mather

* Supported by the joint program of the Office of Naval Research and the U. S. Atomic Energy Commission.

† An account of this research has been submitted by G. E. Masek in partial fulfillment of the requirements for the degree of Doctor of Philosophy to the Department of Physics, Stanford University.

[1] B. McDiarmid, Phil. Mag. **46**, 177 (1955); **45**, 933 (1954).
[2] G. D. Rochester and A. W. Wolfendale, Phil. Mag. **45**, 980 (1954) [reviewing data of M. L. T. Kannangara and G. S. Shrikantia, Phil. Mag. **44**, 1091 (1953)].
[3] W. L. Whittemore and R. P. Shutt, Phys. Rev. **88**, 1312 (1952).
[4] Amaldi, Fideraro, and Mariani, Nuovo cimento **7**, 553 (1950).
[5] E. Amaldi and G. Fideraro, Helv. Phys. Acta **23**, 93 (1950); Phys. Rev. **81**, 339 (1951).
[6] B. Leontic and A. W. Wolfendale, Phil. Mag. **44**, 1101 (1953).
[7] George, Redding, and Trent, Proc. Phys. Soc. (London) **A66**, 533 (1953).
[8] E. P. George and P. Trent, Proc. Phys. Soc. (London) **A64**, 1134 (1952).
[9] W. Heitler, *Quantum Theory of Radiation* (Clarendon Press, Oxford, 1954), third edition, p. 257.
[10] G. Wentzel, Phys. Rev. **79**, 710 (1950); Progr. Theoret. Phys. (Japan) **5**, 584 (1950).
[11] V. L. Fitch and J. Rainwater, Phys. Rev. **92**, 789 (1953).

et al.[12] and by Feld *et al.*[13] In both cases only limits on the cross section could be established in excess of the predicted value. The work of Feld *et al.*[13] set a limit of twenty times the predicted value, which is sufficient to rule out the cross section predicted by μ-pair theories of nuclear forces.[10]

II. GENERAL DISCUSSION OF THE EXPERIMENTAL METHOD

Several experimental methods were investigated before the method used was adopted. Methods using direct or indirect coincidences between both pair members proved to be impractical because of background and counting-rate difficulties; and instead a method was adopted which could identify the process through a single member of the pair. An experiment seeking direct coincidence between both members of the pair would be extremely difficult with the Mark III linear accelerator.[14] In order to achieve reasonable counting rates, it is necessary to use almost maximum beam current; because of the low duty cycle (60 pulses per second, 0.1- to 0.6-μsec pulse length), this gives rise to large background through the piling up of prompt secondary processes; the direct muon coincidences would have to be observed during the beam pulse, and the coincidences would then be obscured by the prompt background.

Also investigated was the possibility of making coincidences between the electrons and positrons, the decay products of the μ^- and μ^+ mesons, respectively. These decay products can be detected several microseconds after the beam pulse, thus reducing the prompt-background problems. However, the principal source of background is now caused by muons from $\pi-\mu$ decays. It is impossible to separate these muons from μ-pair fragments and retain sufficient counting rates. In the negative channel this background is not serious for the final stopping material will capture negative pions, not allowing their decay into muons; but in the positive channel almost all the pions stopped give rise to muons that are indistinguishable from the muons from pair production. Again, if reasonable counting rates are to be realized, the positive-pion background becomes so large that it gives more than one count per machine pulse, thus precluding discrimination of the coincidence.

Because of this inability to use coincidences between either the μ-meson pairs or their decay products, characteristics of the pair-production process that might allow detection of *single* members of the pair were sought. The only competing process also yielding single muons is the $\pi-\mu$ decay process. As stated above, muons from π decays cannot be separated cleanly from muons from pair production without a large sacrifice

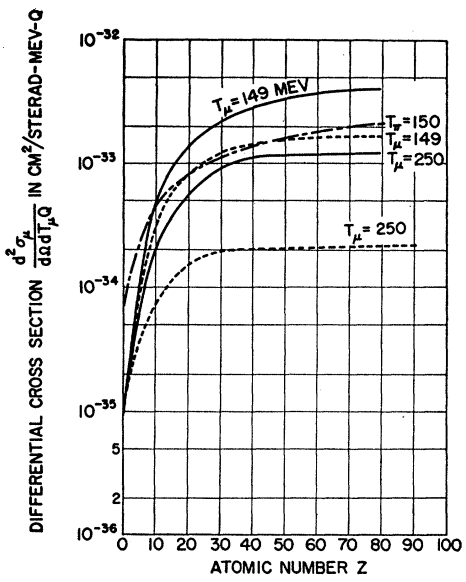

FIG. 1. Curves of the differential cross section for the electromagnetic production of single muons from μ-pair production per effective photon at 10° as a function of the atomic number Z, for various values of the meson kinetic energy and maximum photon energy. All curves were calculated from the mass-scaled Bethe-Heitler equation with a correction for finite nuclear size, and assuming $N(k)=Q/k$ for the bremsstrahlung distribution. The dotted curves are for $k_{max}=500$ Mev, the solid curves for $k_{max}=550$ Mev. The dot-dash curve shows, for comparison, the differential photopion cross section per equivalent photon, assuming an $A^{\frac{1}{3}}$ dependence of the cross section on the atomic weight, and multiplied by the factor 0.01 to enable a comparison.

in counting rate; hence, the production characteristic chosen must differentiate between μ-pair and photopion production. To investigate this, a "predicted" differential cross section for the production of single μ mesons had to be calculated. G. Rawitscher has carried out this calculation by integrating the mass-scaled differential Bethe-Heitler formula[9] over the variables of one pair member, while holding the variables of the other member constant.[15] The variables held constant were the momentum p_-, the angle θ_- between the direction of p_- and the direction of the incident photon, and the photon energy k. The variables of integration were θ_+ and the azimuthal angle ϕ. Larger momentum transfers occur with the μ meson than with electrons of the same energy; therefore it was necessary to correct the point-charge calculation by including a form factor for finite nuclear size [the nuclear radius used was $r_0=(1.20\times10^{-13}\times A^{\frac{1}{3}})$ cm]. The screening effect of the atomic electrons can be neglected since the high momentum transfers make the effective impact parameters small. By folding the results obtained for different values of k into the bremsstrahlung distribution in k from an electron of maximum energy k_{max}, the differential cross section

$$d^2\sigma_\mu^-/QdT_\mu d\Omega \qquad (1)$$

[12] Mather, Martinelli, and Jarmie, Phys. Rev. **82**, 973 (1951).
[13] Feld, Julian, Odian, Osborne, and Wattenberg, Phys. Rev. **96**, 1386 (1954).
[14] Chodorow, Ginzton, Hansen, Kyhl, Neal, Panofsky, *et al.*, Rev. Sci. Instr. **26**, 134 (1955).
[15] G. H. Rawitscher, Phys. Rev. **101**, 423 (1956).

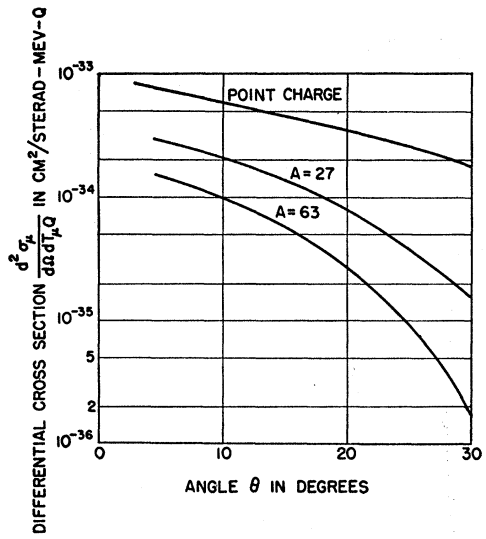

FIG. 2. Curves of the differential cross section for the production of single muons from μ-pair production per effective photon as a function of the laboratory production angle θ, for various values of the atomic weight A; $T_\mu=202$ Mev. All curves were calculated from the mass-scaled Bethe-Heitler formula with correction for finite nuclear size, and using the Bethe-Heitler distribution for the bremsstrahlung of maximum energy 500 Mev. A point-charge curve is also plotted to illustrate the effect of the finite nuclear size on the cross section.

per "effective photon"[16] was obtained. This was done for various values of the atomic number Z of the target material, $\theta(=\theta_-)$, $p(=p_-)$, and $k_{\max}$. Curves of these results are shown in Figs. 1–3.

The dependence of the pair-production process on the Z of the target material was a characteristic we had hoped to be able to use for discrimination; however, it is too similar to the Z-dependence of the photopion process (see Fig. 1). Other characteristics—e.g., meson energy dependence, excitation energy dependence—could presumably have been used, but the one that appears most distinct from the photopion process is the dependence of the pair-production process on the production angle θ. From Fig. 2 it can be seen that the pair-production cross section is strongly anisotropic with respect to the angle θ (increasing in the forward direction). Further, considering theoretical arguments discussed below and our own measurements, there appears to be no appreciable anisotropy in the photopion process for the small range of production angles used in this experiment. Therefore, we chose to examine the variation of the yield of single μ mesons with θ.

The following is a general description of the method used in this experiment (see Fig. 4): The electron beam from the linear accelerator is converted into γ rays by passing it through a converter. The γ rays strike a target from which a variety of particles emerge. These particles comprise, in addition to the electron cascade: (a) pions from photoproduction; (b) muons from $\pi-\mu$ decays in the immediate region of the target; (c) muons from pair production (if the process exists); and (d) nuclear particles from other photoprocesses. The angle of the emerging particles with respect to the γ-ray beam is selected (either $\sim10°$ or $\sim30°$); then the charged particles are momentum analyzed by a magnet M_1 and deflected up a channel. A series of absorbers A_1, A_2, and A_3 in the channel reduces the energy of the particles and brings the meson component of these particles to rest in A_3. In this final absorber A_3 the mesons are either captured or they decay. If they decay, their final decay products (electrons or positrons) emerge into a scintillation-counter telescope. The pulses from the counter telescope are then "counted" through time gates set to observe the characteristic μ-meson half-life.

Although this experimental method is simple in outline, inherent difficulties complicate it and interpretation of the data becomes complex. The most obvious difficulty is the low cross section of the pair process. This makes it necessary to use every means possible to increase the ratio r of the muon yield from pair production to the muon yield from π decay. If the polarity of M_1 is chosen to accept negative particles, pions that come to rest in the final absorber will be captured and no decay electrons will emerge. Thus the pions coming down the channel can yield counts only by decaying in flight. Further, the counts from pion decays in flight can be reduced as follows: If M_1

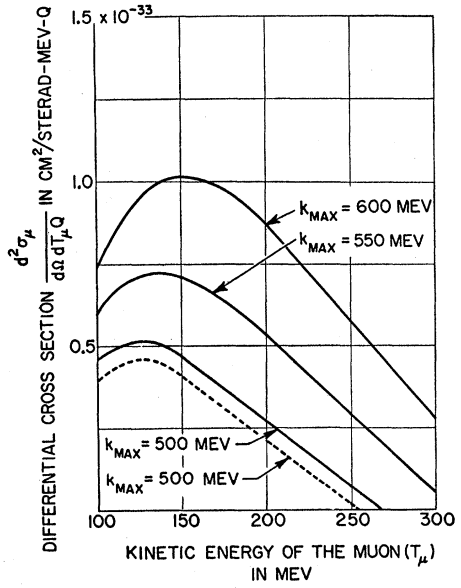

FIG. 3. Curves of the differential cross section for the electromagnetic production of single muons from μ-pair production per effective photon in aluminum at $\theta=10°$, as a function of the muon kinetic energy and for various values of the maximum photon energy $k_{\max}$. All curves were calculated from the mass-scaled Bethe-Heitler formula with a correction for finite nuclear size. The solid curves assume a bremsstrahlung distribution of $N(k)=Q/k$; the dotted curve was calculated from the Bethe-Heitler expression for the bremsstrahlung.

[16] Blocker, Kenney, and Panofsky, Phys. Rev. 79, 419 (1950).

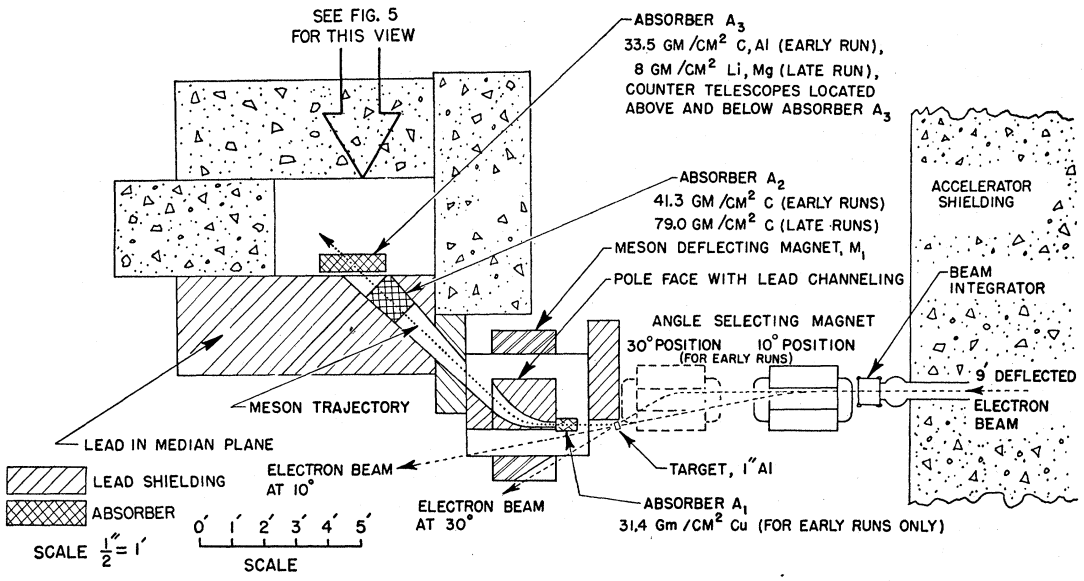

FIG. 4. General experimental arrangement.

passes a meson momentum increment of 10% or less and M_1 is set properly (this will henceforth be called the "μ setting"), it is possible, by making use of the range difference, to stop practically all the pions in absorber A_2, while permitting almost all the muons to pass. Then if A_2 is separated from A_3 by moving A_2 toward M_1, $\pi-\mu$ decays cannot occur in regions near A_3 where the muon detection efficiency would be high. Several other methods can be used to increase the ratio r (as discussed below).

Major difficulties also arise from two other sources of background: (1) An alternate method of producing pions gave an additional source of background in some of the earlier runs. At the time of these runs, absorbers A_1 and A_2 were coupled together into a single absorber (which will be called A_2' for the purposes of this discussion); A_2' had the same stopping power as A_1 and A_2 combined and was placed in the position of A_2. In the 10° position, electrons from the primary beam can be scattered into the entrance of the meson channel by the target. In passing through the target they can lose sufficient energy by radiative straggling to allow them to be accepted by M_1 and to travel down the channel. These electrons would then radiate in A_2' and the photons produced would make pions in A_3. Finally, some of the positive mesons produced would be reabsorbed in A_3 and give rise to background counts.[17] (Aside from the straggling of the primary beam, electrons of the right momentum can also come from electron-pair production in the target.) This method of pion production can be eliminated by splitting A_2' into the two absorbers A_1 and A_2, and placing A_1 in front of the analyzing magnet M_1, thus reducing the energy defined by the meson channel to below threshold for pion production. Mesons of the same initial energy as before first lose energy in A_1, then pass into the channel of M_1 (which is now set to accept lower energies), lose additional energy in A_2, and finally come to rest in A_3, as before. On the other hand, electrons that previously produced pions in A_3 will radiate and lose energy in A_1, and be deflected by M_1 into A_2 where they will also radiate and lose energy; but the photons produced in A_1 cannot geometrically see A_3, and the photons from A_2 are now too low in energy to produce many pions in A_3.

(2) The most serious difficulty comes from the various sources of background, other than pion decays, that occur after the beam pulse. These sources could presumably be radioactivity, photomultiplier afterpulses, etc., but because this background gives real coincidences in the telescopes, it is almost certain that the principal mechanism is from slow neutrons.[18] Further, the magnitude of this background depends on whether the setting is in the 10° or the 30° position, and whether the target is in or out. Hence, we can neither subtract "30° counts" directly from "10° counts," nor "target-out counts" directly from "target-in counts." It is possible to separate this background from the μ^- counts in each running condition by using two different materials interchangeably for A_3. The muon lifetime for nuclear absorption is approximately proportional to $1/Z^4$ of the stopping material; hence, there will be many more decay electrons from a carbon

[17] To check this mechanism, aluminum and carbon absorbers can be used interchangeably for A_3 (described below).

[18] Large numbers of neutrons are made during the beam pulse. By diffusion processes these neutrons can end in the scintillators several microseconds after the beam pulse and cause, e.g., (n,γ) reactions. These γ rays in turn can give rise to electrons with sufficient energy to give counts in the scintillation-counter telescope.

A_3 than from an aluminum A_3 of the same g/cm^2 and otherwise equal physical size. From this difference in the counting rates between a carbon and an aluminum A_3 (or between a magnesium and a lithium A_3), the counts attributable to muons only can be determined. Notice also that the observed half-life of the decay in the case of a high-Z (aluminum or magnesium) A_3 aids in identifying the background.

It is now possible to see how counts attributable to electromagnetic production of muons can be determined. The following statements and assumptions are made: (a) The pion cross section is nearly isotropic in the energy region of 200 Mev between 10° and 30°; and the deviation from isotropy can be measured. (b) The electromagnetic yield of muons should be much greater at 10° than at 30°. (c) The only sources of muons are from pion decays in flight and from direct electromagnetic production. Then if at any particular setting of angle and magnet the counts obtained with an A_3 of high atomic number (Al or Mg) are subtracted from the counts with an A_3 of low atomic number (C or Li), the counts attributable to muons only can be determined from the remainder. Such a subtraction made with M_1 at the μ setting, and in the 30° position, should yield primarily counts attributable to pion decays in flight; in the 10° position, such a subtraction yields, in addition to pion decays in flight, a large contribution of muons from pair production as compared to 30°. Hence, a comparison of the "30°, C-Al (Mg-Li) difference" from the "10°, C-Al (Mg-Li) difference" should give the single muons from pair production.

III. EXPERIMENTAL ARRANGEMENTS, EARLY RUNS

The electron beam of the Mark III linear accelerator was momentum-analyzed by a system of magnets[19] and brought to a $\frac{1}{2}$-in. diameter spot focus in the experimental area. Here the beam was first monitored by a secondary emitter[20] and then deflected by a magnet whose position could be changed along a line parallel to the initial beam line. By deflecting the beam into the target from different magnet positions, it was possible to keep the target and detector geometry fixed and vary the angle θ (see Fig. 4).

We used the highest beam energy available for three reasons: (1) The μ-pair total cross section increases almost quadratically with beam energy, while the photopion cross section increases only slightly; this increases the ratio r. (2) The pair cross section as a function of meson energy peaks at about $T_\mu=\frac{1}{2}(k-2\mu)$ (see Fig. 3); hence higher beam energies allow a higher meson energy to be used. This also increases the ratio r, for the photopion cross section decreases with increasing meson energy.[21,22] (3) The additional absorber necessary to bring higher energy mesons to rest allows greater attenuation of the pions in flight by nuclear absorption; this once again increases r, for the muons experience no nuclear absorption. During the experiment the highest beam energy available was 575 Mev. The muon kinetic energy was near 190 Mev.

After the beam emerged from the beam-deflecting magnet, it passed through a 0.020-in. tantalum converter and then through a 1-in. aluminum target placed immediately behind the converter. The choice of target was a compromise between two considerations: On the one hand, the maximum number of radiation lengths of the target is limited because the primary energy of the electron beam and the resultant γ rays degenerate in traversing the target. The electrons can lose energy by radiative straggling, while the γ rays are absorbed principally through the secondary process of electron-pair production. As mentioned earlier, the μ-pair cross section is a steep function of the primary electron or γ-ray energy, and hence this degeneration causes a decrease in the μ-pair yield. The degeneration does not, however, appreciably affect the pion yield. Therefore, the ratio r decreases as the number of radiation lengths of the target is increased. The maximum tolerable number of radiation lengths for the target was calculated to be $\sim$0.3. The highest absolute yield is then obtained by making the target of the lowest Z possible since the μ-pair cross sections (Fig. 1) vary much more slowly with Z than radiative processes involving electrons. On the other hand, the physical dimensions of the target become too large for a too-low-Z material. Aluminum was used because it gives the best compromise between physical dimensions and low Z. One further consideration limiting the use of too large a number of radiation lengths is that during the beam pulse a large number of ionizing particles reach the scintillators through secondary processes. These par-

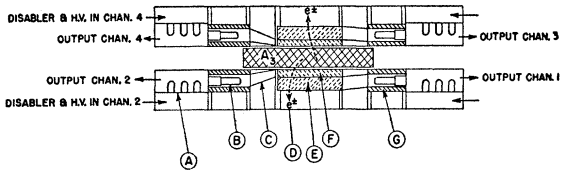

FIG. 5. Vertical cross section through the counters and the last absorber A_3. The exit of the meson channel is immediately behind A_3, and mesons stopping in A_3 travel in a direction out of the page. The dotted lines (D) indicate typical electron or positron trajectories from A_3 through the scintillators. The remaining letters designate: (A) preamplifier for Channel 2; (B) photomultiplier of Channel 2; (C) air light-pipe from scintillator No. 2 to the phototube of Channel 2; (E) 2-in. plastic scintillator No. 4; (F) 1-in. plastic scintillator No. 2; (G) iron magnetic shield around phototube of Channel 1. All four channels above are identical with the exception of the size and position of the four scintillators and their corresponding light-pipes. All the above components are contained in two light-tight copper boxes shown above and below A_3.

[19] W. K. H. Panofsky and J. A. McIntyre, Rev. Sci. Instr. **25**, 287 (1954).
[20] G. W. Tautfest and H. R. Fechter, Rev. Sci. Instr. **26**, 229 (1955).
[21] Walker, Teasdale, Peterson, and Vette, Phys. Rev. **99**, 210 (1955).
[22] Tollestrup, Keck, and Worlock, Phys. Rev. **99**, 220 (1955).

ticles give rise to extremely large light pulses that render the photomultipliers inoperative for several microseconds after the pulse has passed. The scattering of the primary beam into the meson channel by the target is certainly the main source of these ionizing particles. We have developed an electronic method, described below, of "pulsing off" the photomultiplier high voltage during the beam pulse; but unfortunately this does not completely solve the problem if targets of a large number of radiation lengths are used. Targets of fewer radiation lengths scatter fewer secondaries into the scintillators and thereby reduce this problem.

The meson-analyzing magnet, channel, and absorbers have been described. The scintillation-counter telescopes are shown in cross section in Fig. 5. The mesons enter A_3 in a direction normal to the page; the decay electrons emerge from A_3 passing through either one or the other of the telescopes. The aluminum A_3 is composed of layers of perforated sheet to yield the correct density; A_3 is 15.9 g/cm^2 in the vertical direction. The two inside scintillators are 1-in. plastic, and the

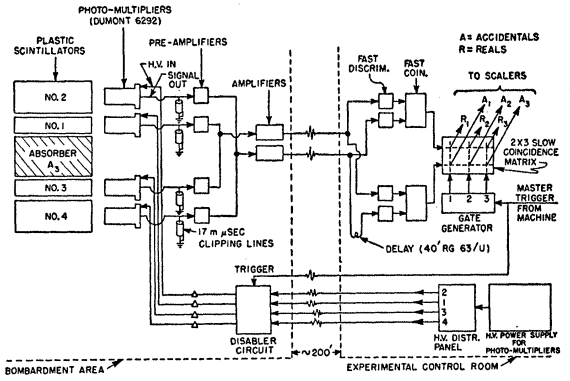

FIG. 6. Block diagram of the electronics used in the experiment.

outside scintillators are 2-in. plastic. All scintillators are viewed by DuMont 6292 photomultipliers, whose outputs are first clipped by 7 ft of Microdot 90-ohm coaxial cable, then amplified by preamplifiers with a gain of 6 and a risetime of 10 mμsec. The outputs from the two inside counters are paralleled, as are the outputs from the two outside counters (Fig. 6). These two signals are amplified further ($\sim$1000 gain, $\sim$20-mμsec risetime). Each output is divided again, yielding four outputs, two of which are the sum of the pulses from the inside counters, and two of which are the sum from the outside counters. Two of these outputs, one inside and one outside, are fed through separate fast discriminators (resolving time 10 mμsec) and then put in fast coincidence (resolving time 20 mμsec). The remaining two are similarly fed through fast discriminators and put in fast coincidence, but one is first delayed by 40 ft of RG-63/U coaxial cable. The outputs of the two coincidence circuits then represent the real and the accidental events, respectively. These outputs are fed into a slow-coincidence matrix which gives coincidences

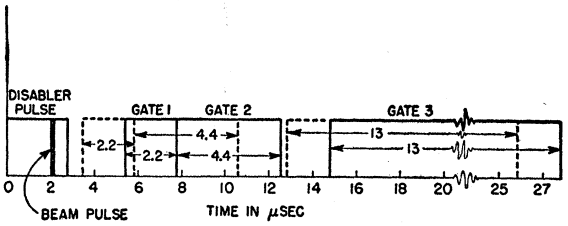

FIG. 7. Timing sequence of electronic operations with respect to the beam pulse. The gates indicated with solid lines give their positions for the early runs; the dotted lines indicate their position for the later runs.

between these signals and three time gates triggered by a pulse controlled by the accelerator time base (Fig. 7). The outputs of the matrix are scaled and counted. The photomultiplier high voltages are pulsed off during the time of the beam pulse by discharging a 3-μsec 50-ohm artificial delay line with a hydrogen thyratron (Fig. 8). The high-voltage disabling pulse was applied not only to the photomultiplier voltage divider but also to a "capacitive cap" (made of copper screen for light-transmission purposes) which covered the photosensitive surface of the photomultiplier; this enabled the photosensitive surface to receive a fast pulse in spite of its relatively high resistivity. A difficulty with this method of pulsing the photomultipliers appeared during the earlier set of runs: The falltime of the pulse was long ($\sim$1.5 μsec), and this introduced nonuniformities in the photomultiplier sensitivity noticeable up to about 8 μsec after the pulse. Thus, whereas the ratio of the counting rates in the first and second gates should have been about 2:1 on the basis of the muon decay lifetime and gate settings, it was in fact 1.7:1. This fall-time difficulty was overcome in the later runs, and the ratio for these runs was very nearly 2:1.

Table I contains a list of all parameters used in the experiment.

IV. EXPERIMENTAL PROCEDURE, EARLY RUNS

The negative-muon cross section was measured relative to the positive photopion cross section. An absolute measurement was not attempted because of uncertainties in many of the experimental parameters, such as the solid angles of the counting system, the momentum acceptance of the meson channel, the counter

TABLE I. Summary of parameters used in experiment.

Parameter	Symbol (if any)	Value Early runs	Late runs
Laboratory production angle	θ	10° or 30°	12° or 23°
Electron beam energy	k_{max}	575 Mev	575 Mev
Kinetic energy of muon observed	T_μ	190 Mev	180 Mev
Absorber 1	A_1	31.4 g/cm^2 Cu	...
Absorber 2	A_2	41.3 g/cm^2 C	79 g/cm^2 C
Absorber 3	A_3	33.5 g/cm^2 C or Al	8 g/cm^2 Li or Mg
Target	...	1.0-in. Al	1.0-in. Al
Radiator	...	0.020-in. Ta	0.020-in. Ta

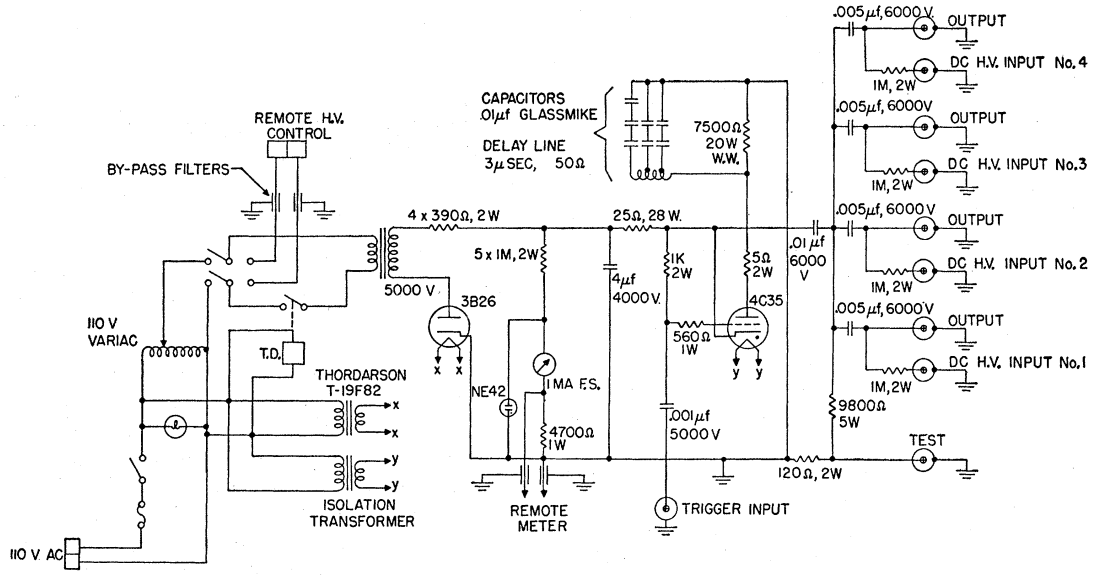

FIG. 8. Circuit diagram of the "disabler" circuit used to pulse the high voltage off the photomultipliers during the beam pulse.

efficiencies, etc. However, by leaving out absorbers A_1 and A_2, setting M_1 to pass positive pions of 70-Mev kinetic energy, and making a number of corrections (described below), we obtained the yield of 70-Mev pions photoproduced in the aluminum target and detected by the setup described. This type of run will be referred to as a Reference-I run (abbreviated as "Ref-I"). In a separate experiment, described below, the photopion cross section of aluminum was compared to the cross section of hydrogen, whose value is known.[23] By comparing the muon yield to the pion yield, an experimental value for the cross section for electromagnetic production of muons was found.

The muon yield due to pair production was found in a series of runs of 10° carbon, 10° aluminum, 30° carbon, and 30° aluminum, as outlined above. These runs were first normalized to the beam current, which was monitored by the secondary emitter and integrated electronically[20]; then they were normalized to a "Ref-II" run in order to guard against possible drift of the counting electronics. A Ref-II run was made by removing A_1 and setting M_1 so that positive pions from the target were brough to rest in A_3; hence, Ref-II measures the yield of 150-Mev positive pions. Ref-II runs of sufficiently good statistics could be obtained in about 10 minutes of running time; by inserting these between the long (2–3 hours) μ-setting runs, it was possible to observe drifts in detecting efficiencies; and by normalizing all runs to Ref-II runs, to correct for these drifts.

The μ setting of M_1—the setting that allows the μ mesons to stop in the middle of A_3—was determined experimentally in the following manner: A series of runs was made of counts *vs* magnet-current setting. For these runs M_1 was set for positive particles, A_1 was removed, and A_2 and A_3 were replaced by $A_2{}^\pi$ and $A_3{}^\pi$ whose total g/cm^2 was increased from that of A_2 and A_3 in the ratio $(m_\mu/m_\pi)^{-1}$. Removing A_1 and setting M_1 for positive particles allowed us to count positive pions at relatively high rates and with little background. These pions were used to calibrate the response of the $A_2{}^\pi - A_3{}^\pi$ absorber-detector system to the setting of M_1. Scaling by m_μ/m_π the momenta accepted by the magnet, an empirical curve of the response to muons could be obtained for the original $A_2 - A_3$ absorber system. Further, from the range-energy relations and the above curves, a pion-response curve can be calculated for A_1 and A_2. These three curves—the experimental pion response with $A_2{}^\pi$ and $A_3{}^\pi$, the scaled muon response with A_2 and A_3, and the calculated pion response with A_2 and A_3—are shown in Fig. 9. By examining the last two curves, it is possible to pick an optimum setting for muon-acceptance and pion rejection.

Other types of runs were made in order to check on various corrections and as checks on the experimental results. These are given in Table II(a), and their significance is discussed below.

V. EXPERIMENTAL ARRANGEMENTS, LATER RUNS

A second series of runs was carried out incorporating some deviations in arrangements and procedures from those previously described: (1) The use of an x-ray beam without passage of the primary beam through the production target (Fig. 10); (2) The use of Mg and Li for A_3; (3) The use of narrower momentum selection $(\Delta p/p = 0.1)$; (4) Omission of A_1. The principal single factor limiting the results from this experiment is our inability to discriminate with a sufficient rejection factor

[23] For a summary of available data, see reference 21, and H. A. Bethe and F. de Hoffmann, *Mesons and Fields* (Row, Peterson and Company, Evanston, 1955), Vol. 2, pp. 144 ff.

against muons from $\pi-\mu$ decay. The changes listed above represent an attempt to overcome this limitation; further steps in this direction are planned.

In principle it is possible to sharpen the resolution of the magnetic spectrometer sufficiently so that no pions pass through A_3. In this series of runs this was achieved by narrowing the spectrometer pass band, and substituting lighter materials for A_3 to stop this narrower energy band of mesons. Lithium was chosen for the low-Z material for A_3 and magnesium (assembled again from perforated sheets) for the higher-Z member. With this arrangement, a curve of counting rate *vs* momentum for positive pions was obtained (Fig. 11), which exhibits considerably better resolution. Figure 11 shows both the measured acceptance curve for pions and the computed curve for muons. As is confirmed by the results, this increased resolution improves the rejection against muons from $\pi-\mu$ decay only slightly since, even though all pions are stopped in A_2 before reaching A_3, muons from decay in flight of pions before being stopped can still reach A_3 with good solid angle. This can be prevented by increasing the separation between A_2 and A_3; however, this leads to increased muon loss due to scattering in A_2, and at low-counting rates this loss could not be tolerated. In future experiments it will be possible, however, to improve rejection by increasing the A_2-A_3 separation.

An x-ray beam was produced by introducing a radiator at an appropriate place in the beam-deflecting magnet (Fig. 10); the electron beam manages to miss both the production target and the magnetic return yoke of the magnet M_1. This method of bombardment improves conditions since (a) the effective bremsstrahlung spectrum is less rounded at its upper limit due to less radiative degeneration of the primary electron beam, and (b) the electrons entering the magnetic channel of M_1 due to scattering of the primary electron beam in the production target are absent. For the latter reason the absorber A_1 becomes unnecessary; hence, the effect of scattering in A_1 on magnet resolution and intensity is removed.

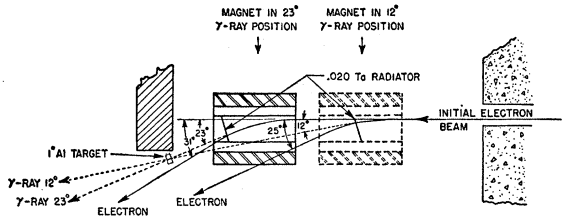

FIG. 10. Diagram showing the layout of the angle-selecting magnet for the later runs in which a γ-ray beam was produced at the tantalum converters and directed into the target, while the remaining electron beam was swept away from the target.

VI. EXPERIMENTAL PROCEDURE, LATER RUNS

The experimental procedure in these runs was identical to that of the earlier runs with two exceptions: The reference count (here called "Ref-III") used to check possible instabilities was taken without change in absorbers from the muon runs; hence no additional measurements on the energy dependence of pion production were necessary. These reference counts were of course slow, thus reducing the over-all data-taking rate. Second, the angles chosen here were 12° and 23°; these were defined by geometrical limitations and the characteristics of the beam-deflecting magnet. Table II(b) shows the data obtained in this set of runs.

VII. SUMMARY OF THE DATA AND EXPERIMENTAL RESULTS

Tables II–V contain summaries of the data, the calculations, corrections, and experimental results.

The data [Table II(a) and (b)] are divided according to the singular significance of a set of runs. A description of each run is given—the absorbers used, angle settings, magnet settings, etc.; each run is designated by a

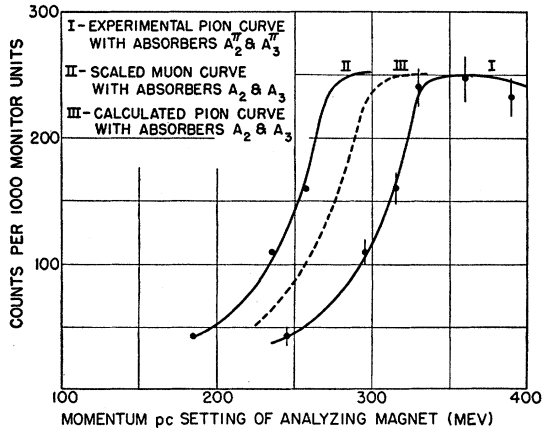

FIG. 9. Curves for the early runs showing the response of the detector-absorber system to mesons of different momenta. The absorbers indicated are described in the text. The "μ setting" was at $pc\sim275$ Mev.

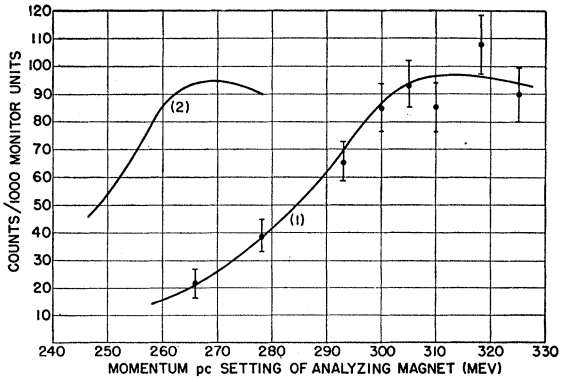

FIG. 11. Curves for the later runs showing the response of the (A_2 and A_3) absorber-detector system to mesons of different momenta. Curve (1) is the experimental response to positive pions; curve (2) is the computed response for muons. For both curves, the absorber A_2 was 79 g/cm² of carbon, and A_3 was 8 g/cm² of lithium.

TABLE II. Data summary. (The entries under M_1 give the meson investigated and its kinetic energy in Mev.)

(a) Early runs

No.	Name of run or purpose as used in text		M_1 (Mev)	θ (degrees)	Absorbers A_1	A_2	A_3	Counts per 1000 Ref-II counts	Total counts
		1						50.9±3.1	378
a	10°, carbon	2	190, μ^-	10	in	in	C	53.0±4.5	158
		3						72.0±3.5	903
		4						59.0±4.1	356
		1						19.0±1.9	114
b	10°, aluminum	2	190, μ^-	10	in	in	Al	22.8±2.8	84
		3						27.6±2.5	235
		4						28.4±3.14	157
		1						55.8±2.74	584
c	30°, carbon	2	190, μ^-	30	in	in	C	38.2±3.2	156
		3						46.0±3.0	317
		4						42.4±2.2	455
		1						32.6±3.1	174
d	30°, aluminum	2	190, μ^-	30	in	in	Al	14.0±2.3	44
		3						11.6±1.1	131
		4						12.3±1.5	97
e	Ref-II (aluminum)		150, π^+	10 and 30	out	in	Al	}	
f	Ref-II (10°)		150, π^+	10	out	in	C	} See Table II(c)	
g	Ref-II (30°)		150, π^+	30	out	in	C	}	
h	Ref-I		70, π^+	10 and 30	out	in	C	3440±19	1584
i	Decay in flight		150, π^+	10 and 30	out	in	C	1000±33	856
j	Decay in flight		150, π^-	10 and 30	out	in	C	170±8.2	458
k	A_1 scattering		210, π^+	10	Be	in	C	422±51[a]	
l	A_1 scattering		210, π^+	10	Cu	in	C	344±45[a]	

(b) Later runs

No.	Name of run or purpose as used in text	M_1 (Mev)	θ (degrees)	Absorbers A_1	A_2	A_3	Counts per 1000 Ref-III counts	Total counts
a'	12°, lithium	180, μ^-	12	out	in	Li	149.0± 8.9	343
b'	12°, magnesium	180, μ^-	12	out	in	Mg	60.6±10.4	38
c'	Ref-III (12°, lithium)	210, π^+	12	out	in	Li		807
d'	Ref-III (12°, magnesium)	210, π^+	12	out	in	Mg		(249)[b]
e'	23°, lithium	180, μ^-	23	out	in	Li	119.0± 9.6	215
f'	23°, magnesium	180, μ^-	23	out	in	Mg	64.0±11.3	37
g'	Ref-III (23°, lithium)	210, π^+	23	out	in	Li		458
h'	Ref-III (23°, magnesium)	210, π^+	23	out	in	Mg		(388)[b]
i'	Ref-I	70, π^+	23	out	out	Li	11 300(±10.4%)[a]	1270±37
j'	Ref-I	70, π^+	23	out	out	Mg	10 700(±10.4%)[a]	1205±37

(c) π^+ yields at pion kinetic energies of 150 and 200 Mev accumulated over both running periods.

Run type	Counts per 1000 monitor units 30°	Counts per 1000 monitor units 10°	$\frac{\sigma_{10°}}{\sigma_{30°}}\Big\vert T_\pi = 150$ Mev
Early runs	1070±21	1062±34	0.995±0.038
Ref-II	2300±52	1982±64	0.863±0.034
carbon	2300±76	2290±57	0.996±0.041
	1300±29	1210±45	0.931±0.040
Early runs	890±23	825±23	0.928±0.036
Ref-II	1570±54	1470±57	0.936±0.049
aluminum	2250±75	1980±70	0.880±0.043
	970±40	975±29	1.004±0.051
		Weighted average:	0.993±0.014

Run type	Counts per 1000 monitor units 23°	Counts per 1000 monitor units 12°	$\frac{\sigma_{12°}}{\sigma_{23°}}\Big\vert T_\pi = 210$ Mev
Later runs Ref-III lithium	147±5.4	134±4.0	0.91±0.04

[a] Counts per 1000 monitor units.
[b] Counts taken with lithium A_3 and reduced to magnesium by the data from runs *i'* and *j'*.

TABLE III. Summary of calculations leading to μ^- yield from pairs.

No.	Result	How obtained from data table		Value per 1000 Ref-II counts
	(a) Early runs			
A	μ^- yield at 10° from both μ-pair production and pion decays. Entered separately for each running night.	$a-b$	1	31.9 ± 3.60
			2	30.2 ± 5.36
			3	44.4 ± 4.30
			4	30.6 ± 5.15
B	μ^- yield at 30° from both μ-pair production and pion decays. Entered separately for each running night.	$c-d$	1	23.2 ± 4.1
			2	24.2 ± 4.0
			3	34.4 ± 3.2
			4	30.1 ± 2.7
C	μ^- yield from pairs at 10° minus μ^- yield from pairs at 30°; assuming π^- yield at 10° equal to π^- yield at 30°. Entered separately for each running night.	$A-B$	1	8.7 ± 5.45
			2	6.0± 6.69
			3	10.0 ± 5.35
			4	0.5 ± 5.80
$\bar{C}$	Weighted average of μ^--yields as given in C.			6.56± 2.88
	(b) Later runs			
A'	μ^- yield at 12° from both μ-pair production and pion decays.	$a'-b'$		88.4 ±13.7
B'	μ^- yield at 23° from both μ-pair production and pion decays.	$c'-d'$		55 ±14.8
C'	μ^- yield from pairs at 10° minus μ^- yield from pairs at 23° assuming only that $\left.\frac{\pi^+ \text{ yield}}{\pi^- \text{ yield}}\right\|_{12°,\,180\text{ Mev}} = \left.\frac{\pi^+ \text{ yield}}{\pi^- \text{ yield}}\right\|_{23°,\,180\text{ Mev}}$.	$A'-B'$		33.4 ±20

lower-case letter that is used in the calculation summary [Table III(a) and (b)] to show how the calculations are derived from the data. As mentioned earlier, the data are summarized per 1000 Ref-II or Ref-III counts. The total number of real counts minus the accidental counts (see Fig. 6) is also given for each run. The accidental were usually less than 10% of the real counts and hence contributed only slightly to the statistical error. Runs a, b, c, and d are subdivided to show the data taken during separate nights of running. In analyzing the data, the aluminum (or magnesium) counts are always subtracted from carbon (or lithium) counts of the same subdivision or the same night's run [Table II(a) and (b)]. The summaries then appearing in items A and B of Table III(a) are the averages of all the C-Al differences for each separate night's run weighted by the reciprocal of the square of their standard deviations. (All the data for the later runs with Mg and Li A_3 were accumulated in one night's running.) This insures that the Al (Mg) (background) runs and the corresponding C (Li) (signal) runs were performed under the same conditions. For various reasons the same conditions did not prevail from one night to the next, as can be seen from the data of Table II(c).

Table III(a) and (b) summarizes the calculations made in obtaining the experimental μ-pair yield. The measurements of the various yields are compared to what is called "Ref-II"—the π^+ yield for 150-Mev pions for the early runs—and what is called "Ref-III" —the yield of 200-Mev pions for the later runs.

The principal background in the experiment is the μ^- yield from the decay of negative pions of about 200-Mev kinetic energy. Hence in the reduction of the data it is necessary to establish relations between the yield of 150- and 200-Mev positive pions and the yield of 200-Mev negative pions for the range of production angles investigated. Specifically, we need information on the ratio

$$\left(\frac{\sigma_{\pi^-,\text{200-Mev}}}{\sigma_{\pi^+,\text{150-Mev}}}\right)_{30°} \Big/ \left(\frac{\sigma_{\pi^-,\text{200-Mev}}}{\sigma_{\pi^+,\text{150-Mev}}}\right)_{10°}, \tag{2}$$

for the earlier runs; and the ratio

$$\left(\frac{\sigma_{\pi^-,\text{200-Mev}}}{\sigma_{\pi^+,\text{200-Mev}}}\right)_{23°} \Big/ \left(\frac{\sigma_{\pi^-,\text{200-Mev}}}{\sigma_{\pi^+,\text{200-Mev}}}\right)_{12°}, \tag{3}$$

for the later runs.

There are no direct experimental data available at this time that fully justify the assumption that the π^+/π^- ratio for 200-Mev pions is independent of angle from 10° to 30°. A 10% uncertainty in the variation of this ratio would give a contribution to the uncertainty of the final results for the μ^- yield equal to that of the purely statistical standard deviation of the result for the early runs and an uncertainty of one-third of the standard deviation of the later runs.

Our belief that the variation of the π^+/π^- photoproduction ratio with angle is substantially less than 10% is based on the following arguments: (1) The experiments of Sands, Teasdale and Walker[24] give a

[24] Sands, Teasdale, and Walker, Phys. Rev. **95**, 592 (1954).

TABLE IV. Corrections applied to Ref-I yield to allow a comparison with the μ^- yield.

(a) All correction factors

No.	Correction	Early runs Value	Early runs Log$_e$	Later runs Value	Later runs Log$_e$
1	A_1 scattering	0.49±0.17	−0.711±0.347	...	...
2	A_2 scattering	0.91±0.045	−0.095±0.050	0.96±0.05	−0.039±0.052
3	Nuclear absorption of pions in A_3	1.33±0.12	+0.292±0.089	1.37±0.12	+0.308±0.087
4	Pion decay in flight	1.21±0.05	+0.190±0.041	1.21±0.05	0.190±0.041
5	(Energy acceptance μ)/(Energy acceptance π)	1.68±0.24	+0.518±0.143	1.95±0.27	0.667±0.139
6	Nuclear absorption of pions in target	1.05±0.03	+0.049±0.029	1.05±0.03	0.049±0.029
7	Loss of muons due to M_1 setting off peak	...	...	0.90±0.05	−0.096±0.056
8	Mean-life difference of positive and negative muons in C and Al (Mg and Li)	0.75±0.03	−0.291±0.040	0.79±0.03	−0.247±0.038
Total factor		0.95±0.20	−0.048±0.39	2.32±0.190	0.842±0.190

(b) Separate summary of pertinent parameters in the A_2-scattering correction (Item No. 2, above)

Run	Run	A_2 (carbon)	$\langle\alpha\rangle^2\times10^4$	Scattering loss in A_2 (%)	Net correction (%)
μ^-	Early	41.3 g/cm^2	4.2	9.0	9.0
Ref-I	Early	...	...	...	
μ^-	Late	79 g/cm^2	10.7	14.5	4.0
Ref-I	Late	14 g/cm^2	5.5	10.5	

value of the π^-/π^+ ratio for the photoproduction of 200-Mev pions in deuterium of 1.18 at 73° and 1.01 at 27°. Theoretically there is essentially no mechanism other than Coulomb effects for a π^-/π^+ ratio less than unity for the deuteron since there is a recoil current in the case of π^- production but not in the case of π^+ production. Therefore we believe that the +/− ratio in deuterium cannot undergo appreciable variation in the angular range $0<\theta<30°$.

For more complex nuclei the situation is not entirely clear at this time, but as far as this problem is concerned our understanding is probably adequate.

In a heavy nucleus one can neglect the energy of the recoiling nucleus. Hence for a given photon energy k and a given pion energy E_π the energy of the final nucleon in the basic processes $\gamma+p\rightarrow n+\pi^+$ and $\gamma+n\rightarrow p+\pi^-$ is defined solely by energy conservation between E_π, k, and the difference in binding energy between the initial and final nuclides. In particular, the angle of emission of the pair does not affect the final energy of the neutron or proton, respectively.

The π^-/π^+ ratio presumably depends on the following factors: (i) The ratio of cross sections of the two basic processes on the free nucleon; (ii) The Coulomb effect of the nuclear charge on the emitted final nucleon; (iii) The difference in the energy available between the initial and final nucleus in case either a π^+ or π^- is created. We have discussed the first factor in relation to the deuteron. The remaining factors (ii) and (iii) will not produce any variation of the π^-/π^+ ratio with pion angle since they depend only on the energy changes involved and on the velocity of the final nucleon; as discussed above, the pion angle does not affect either of these.

(2) The angular variation of the production cross section of each pion (*not* of the π^-/π^+ ratio) will be sensitive to the momentum distribution functions of the nucleons in the initial nuclide. Theoretical integrations based on the assumption of constant final nucleon energy for given pion and photon momenta and using various momentum distributions of the initial nucleons are being carried out in this laboratory.[25] The results obtained thus far indicate a ratio of $\sigma_{10°}/\sigma_{30°}$ of somewhat less than unity. This is borne out by our measurements as tabulated in Table II(c). This table summarizes the data on π^+ yields at 150-Mev and 190-Mev pion energies at angles of 10° and 30°, and 12° and 23°. As the result of these runs we obtain

$$(\sigma_{10°}/\sigma_{30°})_{T\pi^+=150\text{ Mev}}=0.98\pm0.02, \quad (4)$$

$$(\sigma_{10°}/\sigma_{30°})_{T\pi^+=200\text{ Mev}}=0.92\pm0.06, \quad (5)$$

in qualitative agreement with the above arguments.

Table IV(a) summarizes the corrections applied to the experimental pion yield (Ref-I runs) to allow a comparison of the pion and μ-pair yields. These corrections are based on the following considerations: (1) A_1 scattering correction. As shown in Table II, Ref-I runs were made without A_1 and without A_2 in the earlier runs, and with only a small value of A_2 in the later runs. The μ-setting runs were made with both A_1 and A_2. Thus, there will be a loss in the μ-pair counting rate due to scattering in A_1 and A_2. The loss from A_1 was determined experimentally by setting M_1 to stop positive pions in the middle of A_3 and comparing the counting rate between a beryllium A_1 and a copper A_1 of the same stopping power. A curve was drawn of counting rate, corrected for the difference in nuclear absorption in the two A_1's ,as a function of $[(X/X_r)/(pv)^2]$, where X/X_r is the number of radiation lengths of A_1, and p is the momentum and v the velocity of the particles (the values used for the mean free paths for

[25] K. M. Crowe (private communication).

nuclear absorption were 59 g/cm² for Be, and 106 g/cm² for Cu). From this curve the scattering loss for A_1 can be calculated. (2) A_2 scattering. The number of mesons lost due to the scattering in A_2 was obtained from the vertical spatial distribution of particles at A_3. This was calculated assuming that the exit face of A_2 was a uniform source of mesons with an angular distribution determined from the multiple scattering of the mesons in passing through A_2. To find the plane mean square multiple scattering angle $\langle\alpha\rangle^2$, we numerically integrated the relation

$$\langle\alpha\rangle^2=\frac{(21.2)^2}{2}\int_{\text{absorber}}\frac{dt}{p^2(t)v^2(t)}, \tag{6}$$

using the notation of Bethe and Ashkin.[26] From this value of $\langle\alpha\rangle^2$, the scattering loss is easily calculated. Table IV(b) tabulates the numerical results obtained. The loss due to the horizontal spatial distribution was estimated to be negligible.

(3) Nuclear absorption of pions in A_3. The pions of Ref-I runs experience nuclear absorption in A_3 while the muons of the μ-setting runs do not. The mean free path for this absorption is taken as 59 g/cm². In the early runs, one-half of the final absorber (17 g/cm²) was used for the path length in the absorber. In the later runs, 14 g/cm² of carbon (placed in the position of A_2) and one-half of A_3 (4 g/cm² of lithium) were effective in absorption of the pions in the Ref-I runs. This gives the correction listed.

(4) Pion decay in flight. The pions of a Ref-I run traverse about 11 ft of air before stopping in A_3. For 70-Mev pions, this amounts to 0.38 mean free path for decay in flight. A large fraction of the muons from pion decays in flight was not counted, for they either had the wrong energy to be stopped in A_3 or missed A_3 geometrically. The number of muons from pion decay in flight that is counted can be obtained from the ratio of the positive- to negative-pion counting rates as given in items i and j of Table II(a) (assuming $\sigma_{\pi^+}/\sigma_{\pi^-}\cong 1$). Thus, 17% of the pion counting rate is due to pion decays in flight, and the pion counting rate can be written

$$N=N(L)+0.17N, \tag{7}$$

where N is the actual pion counting rate and $N(L)$ is the number of pions that have not decayed at a distance L from the target; $N(L)$ can be written in terms of $N(0)$, the number of corresponding pions emerging from the target, by making use of the number of mean free paths for decay in flight, giving $N(0)=1.46N(L)$, and hence $N(0)=1.21N$.

(5) Difference in energy increments due to magnetic momentum selection. The magnet M_1 passes a constant fractional momentum interval; hence for different-energy mesons the energy increment passed will vary as p^2/E. Absorber A_3 was designed not to limit the energy acceptance of the counting system. Therefore, the counting rates for different-energy mesons will vary by the factor $(p^2/E)\times(d^2\sigma/dEd\Omega)$. The pion energy for both the early and late Ref-I runs was 70 Mev, while the muon energy *in the magnet* was 135 Mev in the early runs and 180 Mev in the late runs.

(6) Nuclear absorption of pions in the target. The target offered about 0.05 mean free path for nuclear absorption, giving the correction listed.

(7) Loss in μ-pair yield due to momentum setting (later runs only). In order to realize a better signal-to-noise ratio, it was found desirable to carry out the μ-setting runs at a momentum setting slightly removed from the calculated peak of the momentum curve (see Fig. 11). This introduced a loss of about 10% from the peak rate of the μ-pair yield.

(8) Mean life differences of the muon decay. The pions of Ref-I runs are actually counted through the decay electrons of their decay muons. Because these electron pulses are time-selected by fixed gates delayed with respect to the initial beam pulse, the pion- as well as the μ-setting counting rate is sensitive to the muon lifetime. Ref-I pions are counted through positive muons which have the characteristic muon mean life τ^+ of 2.15 μsec; while all of the μ-setting runs were counted through negative muons whose mean lives are commensurate with the Z of the stopping material. Further, the C−Al and Li−Mg subtractions must be corrected for the finite efficiencies of Al and Mg A_3's for counting negative muons. Both of these effects can be taken into account simultaneously by applying the following correction formula (for early runs):

$$C_8=\frac{f_C[\exp(-t_1/\tau_C^-)-\exp(-t_2/\tau_C^-)]-f_{Al}[\exp(-t_1/\tau_{Al}^-)-\exp(-t_2/\tau_{Al}^-)]}{[\exp(-t_1/\tau^+)-\exp(-t_2/\tau^+)]}, \tag{8}$$

where t_1 is the interval between the start of Gate I and the time of the beam, and t_2 is the interval between the end of Gate II and the time of the beam; τ_C^- and τ_{Al}^- are negative-meson mean lives for decay in carbon and aluminum, respectively, and are taken to be 1.96 and 0.812 μsec; f_C and f_{Al} are the fractions of muons which decay—0.907 in carbon and 0.326 in aluminum. A similar expression applies for the later runs, where the C and Al subscripts are replaced by Li and Mg, and the corresponding values become $\tau_{Li}^-=2.12$ μsec, $\tau_{Mg}^-=0.95$ μsec, $f_{Li}=0.98$, and $f_{Mg}=0.44$.

The errors to the correction factors listed in Table IV(a) are estimates based on all the known uncertainties entering into the above calculations and measurements.

[26] H. A. Bethe and J. Ashkin, in *Experimental Nuclear Physics*, edited by E. Segrè (John Wiley and Sons, Inc., New York, 1953), Vol. 1, pp. 283 ff. The quantity pv is in Mev and t in radiation lengths.

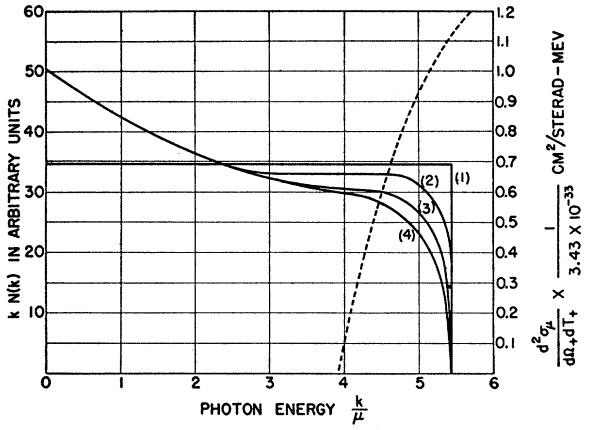

FIG. 12. Bremsstrahlung-distribution curves as a function of the photon energy with a maximum photon energy of 575 Mev. Curve (1) assumes $kN(k)$=constant. Curve (2) is the thin-target distribution calculated from the Bethe-Heitler formula. Curve (3) is the effective thick-target distribution for producing mesons in a 1-in. aluminum target when bombarded by bremsstrahlung produced in a 0.020-in. tantalum converter. The straggling due to radiative degeneration of the primary electron beam in the radiator is taken into account. Curve (4) is the effective thick-target distribution for producing mesons in a 1-in. aluminum target and a 0.020-in. tantalum converter when bombarded by an electron beam of maximum energy 575 Mev degenerated by passage through both the radiator and target. The dotted curve shows the μ-pair-fragment cross section in aluminum per photon as a function of the photon energy, for T_μ=202 Mev, and θ=10°. (The ordinate at the right applies to the dotted curve.)

As mentioned above, the thick target degenerates the energy of the electron beam passing through it and also absorbs a fraction of the photons produced in the target. The μ-pair yield is strongly dependent on the maximum excitation energy, while the pion yield is not. Therefore, the thick target lowers the μ-pair yield relative to the pion yield. The electron degeneration was calculated from the energy distribution formula for radiative straggling as given by Heitler.[27] The target and radiator dimensions are as shown in Table I. The results of these calculations are shown in Fig. 12. The theoretical μ-pair cross sections applying to each type of run have been integrated over the appropriate thick-target spectra and the resulting integrals constitute the theoretical comparison cross sections assumed in Sec. IX.

VIII. PION CROSS SECTION IN ALUMINUM

The pion cross section in aluminum was measured in a separate experiment employing the experimental setup used in other meson-production experiments in this laboratory.[28,29] The angle used was 30°, the meson kinetic energy was 70 Mev, and two electron-beam energies were employed—525 and 350 Mev. These are the same conditions under which the Ref-I runs of the μ-pair experiment were made except that the maximum beam energy in the Ref-I runs was 575 Mev (this introduces negligible error). In this experiment the electron beam first passed through a 0.010-in. tantalum converter, and then the electrons and γ rays impinged upon one of three targets used: 0.0865-radiation-length carbon, 0.0522-radiation-length CH_2, or 0.0732-radiation-length aluminum. The positive-pion yields for these three targets are given in Table V. The ratio of the photopion cross section per effective photon in carbon to that in CH_2 can be calculated from the ratio of the C and CH_2 yields. For this calculation the total radiation length effective in producing the photons for the reaction was taken to be the radiation lengths of the converter plus one-half the radiation lengths of the target plus the equivalent radiation lengths for direct electron production[29] (taken to be 0.020). The number of effective photons Q will be directly proportional to the total radiation lengths (provided the total radiation length is less than ~0.20; above this value, thick-target corrections would have to be used). From the ratio of the carbon and CH_2 cross sections and the similarly obtained ratio of the aluminum and carbon cross sections, the ratio of the photopion cross section per Q in Al can be found relative to the cross section per Q in hydrogen for photons of 350-Mev maximum energy. Finally, comparing the Al yields for maximum photon energies of 350 and 525 Mev, the ratio is found for the photopion cross section per Q in Al at k_{max}=525 Mev to the photopion cross section per Q in hydrogen at k_{max}=350 Mev; thus,

$$\left.\frac{d^2\sigma_{Al}}{QdTd\Omega}\right|_{k_{max}=525\text{ Mev}} \Big/ \left.\frac{d^2\sigma_H}{QdTd\Omega}\right|_{k_{max}=350\text{ Mev}} = 10.9\pm1.2. \quad (9)$$

To obtain an absolute value for the aluminum cross section, it is necessary to evaluate (9) in terms of the absolute value for the hydrogen cross section. The

TABLE V. Summary of data and calculations made in obtaining the π^+ cross section in aluminum.

Target	Counts per 400 monitor units at k_{max}=350 Mev	Counts per 400 monitor units at k_{max}=525 Mev
	(a) Data	
Carbon	1851±45	···
CH_2	1798±45	···
Aluminum	778±44	1974±51

(b) Ratio of cross sections

Ratio $d^2\sigma/Q\,dT\,d\Omega$	Value
$\left(\frac{\sigma_H}{\sigma_C}\right)_{k_{max}=350\text{ Mev}}$	1.98±0.14
$\left(\frac{\sigma_{Al}}{\sigma_C}\right)_{k_{max}=350\text{ Mev}}$	2.10±0.13
$\left(\frac{\sigma_{Al}}{\sigma_C}\right)_{k_{max}=350\text{ Mev}}$	4.17±0.39
$\frac{(\sigma_{Al})_{k_{max}=550\text{ Mev}}}{(\sigma_{Al})_{k_{max}=350\text{ Mev}}}$	2.53±0.15

[27] W. Heitler, reference 9, pp. 377 ff.
[28] Crowe, Friedman, and Motz (to be published).
[29] Panofsky, Newton, and Yodh, Phys. Rev. **98**, 751 (1955).

latter is given per photon; hence it is necessary to convert this to the cross section per equivalent photon Q. Let the hydrogen cross section per photon per steradian be $\sigma_{H,\pi}$ and the photon distribution for the bremsstrahlung of maximum energy k_{max} be $N(k)$. Then the hydrogen yield per steradian is given by

$$\frac{Y_{H,\pi}}{\Delta\Omega}=\int_0^{k_{max}}\sigma_{H,\pi}(k)N(k)dk$$
$$=\int\sigma_{H,\pi}(k)N(k)(dk/dT_\pi)dT_\pi. \quad (10)$$

We observe only a small meson energy increment ΔT_π near a pion kinetic energy T_π corresponding to a photon energy k_0. Since

$$Q=\int_0^{k_{max}}kN(k)dk/k_{max},$$

we obtain for the yield per effective photon per steradian per Mev

$$\frac{Y_{H,\pi}}{Q\Delta\Omega\Delta T_\pi}=\sigma_{H,\pi}(k_0)\left(\frac{dk}{dT_\pi}\right)_{k_0}\frac{N(k_0)k_{max}}{\int_0^{k_{max}}kN(k)dk}; \quad (11)$$

the coefficient $(dk/dT_\pi)_{k_0}$ can be evaluated from the kinematics of the reaction, and $N(k_0)k_{max}/\int_0^{k_{max}}kN(k)dk$ can be evaluated using the Bethe-Heitler expression for $N(k)$, and is 4.73×10^{-3} Mev^{-1}. Hence, the differential cross section for Al per effective photon becomes

$$\left.\frac{d^2\sigma_H}{Qd\Omega dT_\pi}\right|_{\substack{\text{aluminum}\\ k_{max}=525\text{ Mev}\\ T_\pi=70\text{ Mev}\\ \theta=30^\circ}}$$
$$=(5.04\pm0.61)\times10^{-2}\times(d\sigma_H/d\Omega)_{\substack{\text{lab}\\ T_\pi=70\text{ Mev}\\ \theta_{lab}=30^\circ}}, \quad (12)$$

using the values[30]

$$(d\sigma_H/d\Omega)_{\substack{\text{c.m.}\\ T_\pi\ 70\text{ Mev}\\ \theta_{lab}=30^\circ}}$$
$$=(7.2\pm1.2)\times10^{-30}\text{ cm}^2/\text{sterad}, \quad (13)$$

and $d\Omega_{c.m.}/d\Omega_{lab}=1.57$, giving

$$\left.\frac{d^2\sigma_\pi}{Qd\Omega dT_\pi}\right|_{\substack{\text{aluminum}\\ T_\pi=70\text{ Mev}\\ k_{max}=525\text{ Mev}\\ \theta_{lab}=30^\circ}}$$
$$=(5.66\pm0.76)\times10^{-31}\frac{\text{cm}^2}{\text{sterad Mev }Q} \quad (14)$$

for the photopion cross section in aluminum.

[30] We are adopting the value of $(7.2\pm1.2)\times10^{-30}$ cm^2/sterad for the cross section of Eq. (13). This is computed from the best fits of the coefficients of the angular distribution as given by Walker *et al.* (reference 21), from the combined data of the groups at Cornell University, the University of Illinois, and the California Institute of Technology. We have included an additional error of 10% to allow for possible errors in beam standardization.

IX. EVALUATION OF THE μ-PAIR CROSS SECTIONS

The electromagnetic-production cross section for the muon can now be evaluated. For the early runs, the experiment measured the difference between the cross sections at 10° and 30°; this is given by

$$\Delta\sigma_{\mu\text{ pair, exp, }10^\circ\text{–}30^\circ}=\sigma_{\mu\text{ pair, exp, }10^\circ}-\sigma_{\mu\text{ pair, exp, }30^\circ}$$
$$=\sigma_{Al,\pi}(Y_\mu/Y_{Al,\pi})(\prod c_i)^{-1}, \quad (15)$$

where Y_μ is the μ-pair yield given in item C of Table III(a); $Y_{Al,\pi}$ is the pion (Ref-I) yield appearing in item h, Table II(a); and $\prod c_i$ is the product of the correction factors [Table IV(a)]; yielding a value of

$$\Delta\sigma_{\mu\text{ pair, exp, }10^\circ\text{–}30^\circ}$$
$$=(11.39\pm4.99)\times10^{-34}\frac{\text{cm}^2}{\text{sterad Mev }Q}, \quad (16)$$

which is to be compared with the theoretical results of Rawitscher[15] for this difference (the relevant thick-target spectra of Fig. 12 are used):

$$\Delta\sigma_{\mu\text{ pair, theor, }10^\circ\text{–}30^\circ}$$
$$=5.6\times10^{-34}\text{ cm}^2/\text{sterad Mev }Q. \quad (17)$$

For the late runs, the experiment measured the difference in the cross sections at 12° and 23°. Here, Y_μ is in item c' of Table III(b), and $Y_{Al,\pi}$ (Ref-I) is given in j' of Table II(b); $\prod c_i$ appears in the second column of Table IV. Thus,

$$\Delta\sigma_{\mu\text{ pair, exp, }12^\circ\text{–}23^\circ}$$
$$=(7.64\pm4.58)\times10^{-34}\text{ cm}^2/\text{sterad Mev }Q. \quad (18)$$

The corresponding theoretical difference in the 12°–23°, 180-Mev cross section is

$$\Delta\sigma_{\mu\text{ pair, theor, }12^\circ\text{–}23^\circ}$$
$$=4.3\times10^{-34}\text{ cm}^2/\text{sterad Mev }Q. \quad (19)$$

The ratio of the experimental to the theoretical difference for the early runs is

$$\left.\frac{\Delta\sigma_{\mu\text{ pair, exp}}}{\Delta\sigma_{\mu\text{ pair, theor}}}\right|_{10^\circ\text{–}30^\circ}=2.03\pm0.89; \quad (20)$$

and the ratio of the experimental to the theoretical difference for the late runs is

$$\left.\frac{\Delta\sigma_{\mu\text{ pair, exp}}}{\Delta\sigma_{\mu\text{ pair, theor}}}\right|_{12^\circ\text{–}23^\circ}=1.78\pm1.07; \quad (21)$$

where the errors included are the statistical errors of the μ-pair yield only. The average of these two ratios weighted by the reciprocal of the square of their

TABLE VI. Errors in absolute cross section.

No.	Error	$\log_e$ of error factor Early runs	$\log_e$ of error factor Later runs
1	Errors in factors in Table IV(a)	± 0.390	± 0.190
2	Statistical error, Ref-I	± 0.060	± 0.100
3	Beam-energy uncertainty	± 0.100	± 0.050
4	Thick-target calculation	± 0.100	± 0.100
5	Angular uncertainty	± 0.050	± 0.050
6	Statistics in σ_π for aluminum	± 0.110	± 0.110
7	Uncertainty in σ_H	± 0.170	± 0.170
	$\log_e$ of total uncertainty	$\pm 0.470 = \pm \log_e(1.60)$	$\pm 0.320 = \pm \log_e(1.38)$

standard deviations is

$$\left.\frac{\Delta\sigma_{\mu \text{ pair, exp}}}{\Delta\sigma_{\mu \text{ pair, theor}}}\right|_{\text{Av}} = 1.93 \pm 0.68. \quad (22)$$

The statistical errors given with the above ratios represent the uncertainty concerning our evidence on the existence of the process of direct electromagnetic muon production.

If we assume the existence of the process, we are interested in the errors—not included in the previous calculation—of the absolute cross-section determination. These errors are in the form of uncertainties in a number of factors; we find it expedient to calculate the logarithms of these factors and thus to establish the uncertainty in absolute cross section in terms of an uncertainty factor.

Expressed as standard errors, we estimate the following uncertainties in the factor affecting the absolute normalization: (1) The total errors of all the correction factors as listed in Table IV(a). (2) The statistical error of the Ref-I yield: 6 and 10% for the early and late runs, respectively. (3) The error introduced by the uncertainty in the beam energy of the accelerator. For the early runs the beam energy was known to about 5%; this introduces about a 10% uncertainty in the normalization. The accelerator magnet system was recalibrated before the later runs, and the energy of the accelerator is now known to about 2%, giving an error in normalization of about 5%. (4) Error introduced from the thick-target calculations: about 10%. (5) Error from the uncertainty in θ ($\pm 1°$): about 5%. (6) The statistical error in the measurement of the aluminum photopion cross section: 11%. (7) Error in the known experimental data on the hydrogen cross section, upon which the absolute experimental value of the μ-pair cross section is based: 17%.

These error factors are summarized in Table VI. As computed there we obtain that the results of the early runs are uncertain to within a factor of 1.60, and the later runs to within a factor of 1.38; we adopt a factor 1.5 for both runs.

X. DISCUSSION

Formally our result indicates that, on the basis of counting statistics alone, there is a significant peak of negative-muon production in the forward direction. The observed yield is in good agreement with the value computed for pair production by photons of spin-$\frac{1}{2}$ particles in the Coulomb field of a nucleus of finite size.[31]

The interpretation of this experiment as definite evidence for the existence of the pair-production process is predicated on the assumptions of (1) the validity of the arguments presented in Sec. VII on the angular behavior of pion production at small angles; and of (2) the absence of any mechanism of *direct* production of *single* muons with a peaked angular distribution. This latter point is reasonably well ruled out by the low capture rates of negative muons and the experiments on mesic x-rays.[11]

In addition to these reservations, the statistical accuracy of the result is at best marginal. For this reason, and also to minimize the importance of the pion angular distribution, it is necessary to continue these experiments with the objective of improving the rejection of muons from π decay.

Irrespective of the conclusiveness of the evidence concerning the existence proof of the μ-pair process, we can draw additional inferences by treating our result as an upper limit on the cross section.

Of interest here is the relation of this work to the experiments on "anomalous" scattering.[1-8] Electromagnetic pair production is treated as a second-order process consisting of (a) interaction of the incident photon with the pair current of the mesons, and of (b) scattering of the (virtual) pair fragments in the Coulomb field of a nucleus of finite radius. If the second process had a cross section in excess of simple electromagnetic scattering, the μ-pair cross section would be increased correspondingly.

A critical discussion of the μ-scattering experiments

[31] The "theoretical" μ^- yield used here ignores contributions from pair production events in which the Coulomb interaction with the nucleus is inelastic. An upper limit on this contribution can be placed by the relation

$$\frac{\sigma_{\text{inelastic}}}{\sigma_{\text{elastic}}} \leq \frac{1}{Z}\frac{1-|F|^2}{|F|^2},$$

where F is the "nuclear form factor" for a given momentum transfer; $|F|^2$ is thus the correction for nuclear size exhibited by the curves of Fig. 1. For production from aluminum at $\theta = 10°$, this equation gives $\sigma_{\text{inelastic}}/\sigma_{\text{elastic}} \leq 0.18$. An additional contribution up to 18% from this source is thus not excluded.

would be inappropriate here.[32] The work of George *et al.*[7,8] describes an excess of large-angle scattering for initial muon energies in the 100- to 300-Mev region. The recent work of McDiarmid[1] obtains agreement with theory in the energy region essentially below 1 Bev, but for both Fe and Pb he reports an excess of large-angle scattering above the theoretical value. By "theoretical value" we mean Coulomb single or plural scattering *including* the effect of nuclear size.[33] The experimental findings[1–8] often are summarized by the conclusion that agreement is reached if the effect of nuclear size is ignored. Whatever the reason for the discrepancy, the fact that agreement with a point electromagnetic interaction is obtained is surely accidental. The momentum transfers to the nucleus involved in our experiment are in the range 200 Mev $>cp>40$ Mev; this is similar to the range in which George *et al.*[7,8] report large anomalous effects. We seem to be in disagreement with their work, as is the recent work of McDiarmid.[1] We cannot make as positive a statement about the high-energy anomalous scattering observed by McDiarmid[1] since there is little overlap in momentum transfer between our work and the "anomalous range" in which McDiarmid observes an excess of large-angle events. Nevertheless, we feel that this experiment makes less likely the explanation of the anomalous scattering in terms of nonelectromagnetic effects.

At this time we can draw no definite conclusion from our result concerning the value of the spin of the muons. Spin-zero, although of course unlikely for other reasons,[34] is not excluded by these measurements although the agreement is fairly poor; the theoretical value[35] is less than the Bethe-Heitler value by a factor of 1.85. Calculations on spin-$\frac{3}{2}$ theories are in progress.[15]

[32] L. N. Cooper and J. Rainwater [Phys. Rev. **97**, 492 (1955)] discuss these experiments critically, and also examine the theories of multiple and plural scattering in a Coulomb field of a nucleus of finite size required in the interpretation of the μ-scattering experiments.

[33] S. Olbert, Phys. Rev. **87**, 319 (1952).

[34] See, for example, the work of F. E. Driggers [Phys. Rev. **87**, 1080 (1952)] concerning the evidence favoring spin-$\frac{1}{2}$ from cosmic-ray experiments on muon-produced bremsstrahlung and electron knock-ons.

[35] W. Pauli and V. F. Weisskopf, Helv. Phys. Acta **7**, 709 (1934). Integration for this case done by G. H. Rawitscher.

ACKNOWLEDGMENTS

Many members of the staff of this laboratory have contributed to this experiment. Principally, Dr. K. M. Crowe, Professor W. M. Woodward, and A. J. Lazarus have contributed assistance and advice on many aspects of the problem. We are grateful to Dr. Crowe in particular for informing us on the experimental and theoretical status of the problem of photopion production in complex nuclei. Dr. J. A. Narud has provided many of the basic electronic designs for the circuits used. Dr. D. C. Hagerman, D. M. Bernstein, and Dr. W. S. C. Williams have given assistance in both the design and execution of the experiment. The accelerator group, under the direction of Professor R. F. Mozley, has been responsible for providing 10^{18} electrons of 575 Mev for this experiment; we are greatly indebted to their cooperation in this respect. We are indebted to G. H. Rawitscher for carrying out his calculation on the integrals over the Bethe-Heitler formula for the specific parameters of interest to this experiment. Our theoretical understanding of this problem has been aided by discussion with Professor D. R. Yennie and correspondence with Professor R. P. Feynman.